
CHAPTER 7

Determination of Membrane Protein Molecular Weights and Association Equilibrium Constants Using Sedimentation Equilibrium and Sedimentation Velocity

Nancy K. Burgess, Ann Marie Stanley, and Karen G. Fleming

T. C. Jenkins Department of Biophysics
Johns Hopkins University
Baltimore, Maryland 21218

Abstract

- I. Introduction
- II. Rationale
 - A. Why Use AUC?
 - B. General Considerations for Sedimentation Equilibrium Experiments of Membrane Proteins
 - C. Special Considerations for Sedimentation Equilibrium Experiments in the Presence of Detergent Micelles
- III. Materials and Methods
 - A. Expression and Purification of Membrane Proteins Used in This Study
 - B. Determination of the Density-Matching Point for C14SB
 - C. Sedimentation Equilibrium Experiments on Membrane Protein Samples Dispersed in C14SB
 - D. Sedimentation Velocity Experiments on OmpF
 - E. Viscosity Measurements
 - F. Density Measurements
- IV. Results
 - A. Analysis of OMPLA Dimerization Energetics
 - B. Analysis of OmpF Trimer Stability in C14SB
 - C. Sedimentation Velocity Experiments on OmpF
- V. Discussion
- VI. Summary
- References

Abstract

Regulated molecular interactions are essential for cellular function and viability, and both homo- and hetero-interactions between all types of biomolecules play important cellular roles. This chapter focuses on interactions between membrane proteins. Knowing both the stoichiometries and stabilities of these interactions in hydrophobic environments is a prerequisite for understanding how this class of proteins regulates cellular activities in membranes. Using examples from the authors' work, this chapter highlights the application of analytical ultracentrifugation methods in the determination of these parameters for integral membrane proteins. Both theoretical and practical aspects of carrying out these experiments are discussed.

I. Introduction

As the number of high-resolution structures of membrane proteins continues to rise, it is increasingly appreciated that integral membrane proteins associate with defined stoichiometries and orientations. In some structures it is easy to rationalize why certain membrane proteins are oligomeric: the potassium channel of the KcsA protein is formed only when four identical transmembrane helical subunits self-associate to create a passageway for the ion (Doyle *et al.*, 1998). In other cases, the underlying functional and physical basis for the oligomeric complex is not as easily understood from the structure. In contrast to KcsA, each monomer of the outer membrane protein F (OmpF) trimer has a pore through which ions can pass; trimerization of OmpF monomers brings them into contact with each other but does not create the physical channel. The underlying physical rationale for trimerization of OmpF is therefore not fully explained by the structural studies alone.

Thermodynamic measurements carried out in solution provide complementary information about the molecular interactions observed in structures. In particular, sedimentation equilibrium analytical ultracentrifugation (AUC) is an extremely useful and accurate method for confirming or invalidating stoichiometries observed in crystal structures (Burrows *et al.*, 1994). Moreover, if a system is reversibly associating in solution, these experiments can additionally provide access to key thermodynamic parameters for the reaction, such as the equilibrium constant; knowing this value, the oligomeric species distribution can be predicted over wide ranges of concentrations, and the biological significance of oligomeric species can be better understood.

Solution studies whose principal aim is to determine the mass or stoichiometry of a protein complex have historically been challenging to carry out on membrane proteins because they reside *in vivo* in the anisotropic, chemically heterogeneous environment of the biological lipid bilayer. Solution studies *in vitro* require manipulation of purified membrane protein samples, and solubility of integral membrane proteins requires that they be handled in the presence of a hydrophobic cosolvent.

In the vast majority of structural studies, this cosolvent is provided by detergent micelles, which introduces complexity into the analysis as this detergent binding contributes to the overall mass of a membrane protein complex and must be taken into account in order to separate the mass contributions of the protein from those of the bound detergent. Any bound lipid that may copurify with a membrane protein will also contribute to its molecular weight. In addition to the contribution of bound detergents and/or lipids to the mass of a membrane protein complex, they affect the shape of the overall complex. Therefore, any experimental method that is fundamentally dependent on transport (e.g., dynamic light scattering, gel filtration chromatography, sedimentation velocity) can be difficult to interpret because the shape contributions of the protein and the bound cosolvent can be difficult to separate from one another (see Chapter 12 by Byron, this volume). In this chapter we will discuss some of the strategies that can be used to overcome some of these technical barriers in analyzing membrane protein complexes dispersed in detergent micelle solutions to determine their molecular weights, interactions, and stoichiometries.

II. Rationale

A. Why Use AUC?

AUC, and in particular sedimentation equilibrium, is an extremely useful method for determining molecular weights of complexes in detergent micelle solutions. The principal advantage of sedimentation equilibrium is that it provides a direct measure of mass. This is in stark contrast to spectroscopic methods, such as fluorescence resonance energy transfer (FRET), which also have been used to evaluate membrane protein interactions. In FRET studies, the experimental quantity that can be obtained is the mole ratio of a particular interaction: the titration curve for a monomer–dimer reaction would appear identical to that for a dimer–tetramer reaction. Furthermore, the absence of an interaction would be experimentally observed as a lack of resonance energy transfer in a FRET experiment. Since there are many spectroscopic reasons why donor fluorophores might not efficiently transfer their energy to acceptor fluorophores, a lack of FRET is essentially a negative and noninterpretable result. In contrast, a lack of interactions (or change in molecular weight) in a sedimentation equilibrium experiment would result in a direct measurement of either the nonassociating monomeric or the nondissociating dimeric molecular weight.

B. General Considerations for Sedimentation Equilibrium Experiments of Membrane Proteins

The general considerations for both sedimentation equilibrium and sedimentation velocity experiments are described in detail in an accompanying chapter of this series (Chapter 6 by Cole *et al.*, this volume). The mechanics of carrying out

experiments with membrane protein samples will be the same as described for soluble proteins in their chapter. One practical difference is that membrane protein samples in detergent solutions can be trickier to pipet into the ultracentrifugation cells as the surface tension of these solutions is lower due to the detergent content.¹ In addition to solubilizing membrane proteins, detergent solutions can also solubilize residual proteins in ultracentrifugation cells that are routinely used for soluble proteins, and it may be prudent to set up cells with detergent-only solutions overnight prior to an experiment in order to “wash” them. As is the case for soluble proteins, the purity of a membrane protein preparation is a key aspect of obtaining the best data possible, and any contaminating material can profoundly complicate the data analysis.

There are also considerations of the detection system to be used in an experiment. For the analysis of membrane protein distributions, we have exclusively used the absorbance optics of the Optima XL-A and XL-I ultracentrifuges to monitor the protein’s radial distribution. We use absorbance optics because the detergents we employ do not absorb light at the wavelengths used to monitor the protein concentration, and therefore their distribution can be isolated from that of other components. While in principle the interference optics system could also be used to observe the protein distribution, the interference signal will contain contributions from both the protein and the bound detergent. Moreover, interference optics will detect any and all differences in the refractive indices between a reference and a sample chamber and may also contain a signal from free detergent. To avoid this, all buffer components should be in dialysis equilibrium with each other; however, this condition can be difficult to attain for membrane protein samples dispersed in detergent micelle solutions because detergent concentrations above the critical micelle concentration (cmc) do not always equilibrate across a dialysis membrane. In addition, for thermodynamic studies in which a membrane protein equilibrium constant is the desired information, it is essential to know the detergent concentration accurately, and measuring detergent concentrations following dialysis is not easily accomplished. Therefore, as an alternative to dialysis for our experiments, we have used a “column exchange” method to establish the solution detergent concentration (described in [Section III](#)).

In contrast to experiments with solubilized membrane proteins, interference optics is actually preferable in experiments where the detergent itself is being

¹ This is especially true for loading the two-sector cells where an air lock can cause the solution to spill over onto the outside of the cell. With both two- and six-sector cells we have found it to be better to place the pipet tip at the bottom of the cell and slowly raise it as the cell fills. In addition, when loading large volumes into two-sector cells, we have found that loading is much easier and more reliable if the entire volume can be injected into the cell at once, and we discovered that using a P1000 pipetman and “piggybacking” a long (round, not flat) gel-loading tip onto the end of the 1 ml blue tip allows the entire volume to be dispersed in one step. Alternatively, BeckmanCoulter, Inc. also manufactures long plastic loading needles that work well for fully loading cells in one step.

characterized. When scanned against a reference sector containing only buffer, detergent micelles are easily visualized by the interference optical system whereas most detergents are not easily detected using absorbance optics. As will be discussed below, when working with a new detergent or in a new buffer, we use interference optics in experiments designed to empirically confirm the buffer conditions required to match the effective density of the detergent micelle.

C. Special Considerations for Sedimentation Equilibrium Experiments in the Presence of Detergent Micelles

1. Buoyant Molecular Weight

To understand and ultimately account for the contributions from the bound detergent, it is important to recognize that the fundamental experimental quantity determined in a sedimentation equilibrium experiment is the buoyant molecular weight (Casassa and Eisenberg, 1964) defined as

$$M_p(1 - \phi'\rho) \quad (1)$$

where M_p is the molecular weight of only the protein portion of the sedimenting particle and excludes the molecular weight of the bound detergent, lipid, and/or water; the quantity $(1 - \phi'\rho)$ is the buoyancy term; ϕ' is the effective partial specific volume (ml g^{-1}) of the protein moiety in the sedimenting particle and takes into account the contributions of the bound detergent, lipid, and water; and ρ is the solvent density. The buoyant molecular weight can be rewritten as a sum of each of the components, and the generalized form of the equation is (Reynolds and Tanford, 1976)

$$M_p(1 - \phi'\rho) = M_p(1 - \bar{v}_p\rho) + \sum n_i M_i(1 - \bar{v}_i\rho) \quad (2)$$

where M_i and \bar{v}_i are the molecular weights and partial specific volumes (ml g^{-1}) of the i th component, and n_i is the number of molecules of any i th component bound to the protein. Any bound components—lipids, detergent molecules, water molecules—will contribute to the buoyant molecular weight, and each of the contributions can be explicitly stated in a specific form of Eq. (2) that can be written as follows:

$$M_p(1 - \phi'\rho) = M_p(1 - \bar{v}_p\rho) + n_{\text{Lipid}}M_{\text{Lipid}}(1 - \bar{v}_{\text{Lipid}}\rho) + n_{\text{Det}}M_{\text{Det}}(1 - \bar{v}_{\text{Det}}\rho) + n_{\text{H}_2\text{O}}M_{\text{H}_2\text{O}}(1 - \bar{v}_{\text{H}_2\text{O}}\rho) \quad (3)$$

where the subscripts Lipid, Det, and H_2O indicate the contributions from the bound lipid, detergent, and water molecules, respectively. This equation is also

often written in the following manner:

$$M_p(1 - \phi' \rho) = M_p[(1 - \bar{v}_p \rho) + \delta_{\text{Lipid}}(1 - \bar{v}_{\text{Lipid}} \rho) + \delta_{\text{Det}}(1 - \bar{v}_{\text{Det}} \rho) + \delta_{\text{H}_2\text{O}}(1 - \bar{v}_{\text{H}_2\text{O}} \rho)] \quad (4)$$

where δ_i represents the amount bound of the i th component in grams per gram of protein. Equations (3) and (4) can be simplified if we assume that the number of bound lipids (n_{Lipid}) is small in a purified-membrane-protein preparation solubilized in detergent micelles at concentrations above their cmc. In this case the buoyant contribution of lipids will be much smaller than the contributions from the bound detergent and can be ignored. This assumption is further justified by the fact that many lipids have partial specific volume values that are close to unity (Durshlag, 1986), which means that the product of $\bar{v}_{\text{Lipid}} \rho$ will also be unity as most buffer densities equal $\sim 1.0 \text{ g ml}^{-1}$. This has the consequence of bringing the buoyancy factor ($1 - \bar{v}_{\text{Lipid}} \rho$) down to a very small number that is essentially equal to zero and thus leads to a negligibly small contribution from bound lipids. This latter argument can also be made for the contribution of water to the buoyant molecular weight as long as the sedimentation equilibrium experiment is carried out in an aqueous solution lacking density additives. Eqs. (3) and (4) can thus usually be simplified in practice to Eqs. (5) and (6), respectively:

$$M_p(1 - \phi' \rho) = M_p(1 - \bar{v}_p \rho) + n_{\text{Det}} M_{\text{Det}}(1 - \bar{v}_{\text{Det}} \rho) \quad (5)$$

and

$$M_p(1 - \phi' \rho) = M_p[(1 - \bar{v}_p \rho) + \delta_{\text{Det}}(1 - \bar{v}_{\text{Det}} \rho)] \quad (6)$$

The principle remaining contribution that must be accounted for is the contribution of the bound detergent, $\delta_{\text{Det}}(1 - \bar{v}_{\text{Det}} \rho)$, to the buoyant mass of the complex.

2. Experimental Strategies to Account for Bound Cosolvent

There are three main strategies that have been used to account for the contribution of the bound detergent or lipid to the buoyant molecular weight. The choice of which strategy to use will depend on the scientific question to be addressed and on the chemical nature of the detergent micelles or lipids that must be used to solubilize the purified membrane protein. These three strategies are (i) measurement and use of the density increment; (ii) explicit accounting for the bound detergent; and (iii) density matching the detergent with the solvent.

a. Density Increment

The density-increment method is especially useful when a membrane protein is dispersed in a chemically heterogeneous detergent/lipid environment. This can occur when a protein copurifies with a significant amount of bound lipid or when the detergent environment that must be used to preserve the protein integrity

cannot be density matched using the methods described below. In sedimentation equilibrium experiments, the density increment is defined as the change in solution density as a function of changing the protein concentration at constant chemical potential (Casassa and Eisenberg, 1964):

$$\left[\frac{\partial \rho}{\partial c_2} \right]_{\mu} = (1 - \phi' \rho) \quad (7)$$

where c_2 is the weight concentration of the protein alone and ϕ' is the effective partial specific volume of the protein in the protein–detergent complex. Note that the right side of equation (7) contains the term $(1 - \phi' \rho)$, which is equal to the buoyancy factor in equation (1). Since the density increment equals the change in solution density as a function of protein concentration ($\partial \rho / \partial c_2$), it is in principle an experimentally accessible quantity and can be measured using a high-precision density meter. The chemical potential subscript, μ , indicates that the protein must be at dialysis equilibrium with all other components; strict adherence to constant chemical potential can in practice be tricky depending on the cmc of the detergent. Nevertheless, even when constant chemical potential cannot be completely ensured, the density-increment approach appears to return molecular weight values that are sensible.

This strategy of accounting for the contribution of the bound cosolvent to membrane proteins has been used extensively by Butler and coworkers with many complex samples (Butler and Kuhlbrandt, 1988; Butler *et al.*, 2004; Konig *et al.*, 1997). In a typical experiment there are two density measurements: (i) the solvent density in the absence of protein (where the solvent contains the appropriate concentration of detergent micelles) and (ii) the density of a protein–detergent (and/or lipid) complex at a known concentration of protein. These two density points are then plotted as a function of protein concentration, fitted to a line, and the slope used as the buoyancy term in converting the experimental buoyant molecular weight into an expression for the molecular weight of the protein alone. Membrane protein complexes with density increments ranging from -0.14 to 0.734 mL g^{-1} have been analyzed using this method (Butler and Kuhlbrandt, 1988; Butler *et al.*, 2004; Konig *et al.*, 1997), and it is particularly suited for the determination of the molecular weight of membrane protein complexes with many constituents.

b. Explicitly Accounting for the Bound Detergent

A second strategy that can be used to account for the contributions of the bound detergent is to explicitly include it; the mathematical expression for this is illustrated by equation (5) above and requires knowledge of two parameters: (i) the number of detergent and/or lipid molecules that are bound and (ii) the partial specific volumes of each of these species. It is usually the case that this second parameter is much better known than the first as the partial specific volumes for a wide variety of detergents and lipids have been measured and tabulated (Durshlag, 1986). In contrast, the knowledge of the number of bound detergents for a

particular membrane protein complex is generally less well known, although le Maire and colleagues have measured detergent binding for a number of proteins and describe protocols to make this measurement using radiolabeled detergent molecules (le Maire *et al.*, 1983, 2000). However, since radiolabeled detergent samples are not generally available, measuring the amount of bound detergent and using this method of disentangling the contributions of the bound detergent from that of the protein is not widely used.

c. The Density-Matching Strategy

“Density matching” is a third strategy that can be used to interpret the experimental buoyant molecular weight in terms of the protein distribution alone. We have favored this approach because the principle goal of many of our experiments has been to determine equilibrium constants for membrane protein interactions; for this we need to know the protein mass as a function of concentration. Since protein complexes of different molecular weights may also bind different amounts of detergent, there are too many parameters to be determined if we must also take into account the detergent binding of each oligomeric complex. The “density-matching” strategy avoids this complication by minimizing the effective contribution of the bound detergent on all protein oligomeric states, and the membrane protein–detergent complex can be analyzed and interpreted just as one would do for a soluble protein in an aqueous buffer.

In the “density-matching” strategy, the experimental conditions are adjusted such that the solvent density is equal to the effective density of the bound detergent molecules in the protein-detergent complex (Reynolds and Tanford, 1976). Mathematically, this is expressed as the condition where $\rho = 1/\bar{v}_{\text{Det}}$. When this is the case, the buoyancy term from the detergent contribution in equation (5) will be a very small number and essentially equal to zero:

$$(1 = \bar{v}_{\text{Det}}\rho) \cong \left[1 = \bar{v}_{\text{Det}} \left[\frac{1}{\bar{v}_{\text{Det}}} \right] \right] = (1 - 1) = 0 \quad (8)$$

When density matching is achieved, the effective contribution of the bound detergent to the experimentally observed buoyant molecular weight essentially becomes zero *no matter how many detergents are bound*, and the detergent is essentially invisible to the centrifugal field generated by the rotational force. The data can then be analyzed in the standard way and interpreted in terms of the protein mass alone.

The “density-matching” strategy works in this straightforward way only when the solvent density is adjusted by using heavy water, and both $^2\text{H}_2\text{O}$ and $^2\text{H}_2^{18}\text{O}$ have been successfully employed. The addition of other cosolvents that increase the solvent density, such as sucrose, affect the chemical potential of water and lead to preferential binding and/or exclusion of water or the additional

cosolvent at the surface of the protein; in this case their contributions to the buoyant molecular weight must be taken into account by the addition of the appropriate terms in [equation \(2\)](#). In other words, cosolvents that increase the solvent density may in fact match the density of the bound detergent, but they simultaneously introduce a mass uncertainty from their own binding and from the preferential binding of water ([Reynolds and Tanford, 1976](#)).

This problem is largely overcome by matching the solvent density with that of heavy water; however, the need to use heavy water means that the chemical nature of detergents that can be used with this strategy is limited. The density of pure $^2\text{H}_2\text{O}$ is 1.1 g ml^{-1} ; therefore, the partial specific volume of the detergent must be between that of water and $^2\text{H}_2\text{O}$, for example, greater than 0.9 and less than unity. Unfortunately, this eliminates a simple evaluation of membrane protein complexes in the frequently employed detergents dodecylmaltoside and β -octylglucoside, since the densities of these detergents are 1.21 and 1.15 g ml^{-1} , respectively ([Reynolds and McCaslin, 1985](#); [Suarez et al., 1984](#)). Even the use of $^2\text{H}_2^{18}\text{O}$ cannot facilitate density matching of these detergents, although Ferguson-Miller and colleagues have shown that careful experiments coupled with a significant density extrapolation can facilitate a mass determination of membrane protein complexes in this detergent ([Suarez et al., 1984](#)). It is also notable that the bile salt detergents have effective densities around $\sim 1.3 \text{ g ml}^{-1}$ and cannot be used at all in density-matching experiments ([Reynolds and McCaslin, 1985](#)). Nevertheless, there are several detergents that can be density matched with $^2\text{H}_2\text{O}$, and these have been extremely useful in evaluating membrane protein interactions. In our early work we used the neutrally buoyant pentaoxyethylene octyl ether (C_8E_5) detergent ($\bar{v} = 0.993 \text{ ml g}^{-1}$) ([Ludwig et al., 1982](#)) to analyze the energetics of the dimerization of the glycoporphin A (GpA) transmembrane helix ([Doura and Fleming, 2004](#); [Doura et al., 2004](#); [Fleming, 1998, 2000, 2002](#); [Fleming and Engelman, 2001](#); [Fleming et al., 1997](#); [Stanley and Fleming, 2005](#)) and the human erbB transmembrane domains ([Stanley and Fleming, 2005](#)). We and others have also used the zwittergent 3-(*N,N*-dimethylmyristyl-ammonio)propanesulfonate, C14SB, and we have used this detergent in our more recent work on transmembrane β -barrels that will be discussed in this chapter ([Ebie and Fleming, 2007](#); [Fleming et al., 2004](#); [Gratkowski et al., 2001](#); [Howard et al., 2002](#); [Kobus and Fleming, 2005](#); [Kochendoerfer et al., 1999](#); [Li et al., 2004](#); [Pinto et al., 1997](#); [Stanley et al., 2006, 2007](#)). C14SB is significantly less expensive than C_8E_5 , and it preserves the native structure and function of our transmembrane β -barrel outer membrane phospholipase A (OMPLA) (Ann Marie Stanley and Karen G. Fleming, unpublished observation). In 20 mM Tris buffer with 200 mM KCl, the density of C14SB was matched by 13% $^2\text{H}_2\text{O}$. In addition, DeGrado and coworkers have employed dodecylphosphocholine (DPC) detergent micelles for several studies exploring both natural and designed transmembrane helix-helix interactions ([Kochendoerfer et al., 1999](#); [Li et al., 2004](#)). DPC requires 52.5% $^2\text{H}_2\text{O}$ to match its density in 50 mM Tris-HCl buffer with 100 mM NaCl ([Kochendoerfer et al., 1999](#)).

III. Materials and Methods

A. Expression and Purification of Membrane Proteins Used in This Study

1. Expression and Purification of OMPLA

The cloning, expression, and purification of OMPLA is described in detail in Stanley *et al.* (2006). Briefly, the amino acid sequence encoding the mature OMPLA protein was cloned into a pet11A-T7 expression vector. HMS174(DE3) cells harboring the expression vector were grown to midlogarithmic phase, and expression of OMPLA was induced for three hours by the addition of 1 mM isopropyl β -D-1-thiogalactopyranoside (IPTG). Cells were harvested, lysed by French press, and inclusion bodies were isolated by centrifugation. OMPLA was refolded, as described by Dekker *et al.* (1997), except that C14SB was substituted for C12SB in all steps. Immediately prior to each sedimentation equilibrium experiment, OMPLA was exchanged into the desired detergent concentration. Instead of dialysis, we have found that the easiest way to do this was to bind the protein to a Q-sepharose column followed by washing the column with five column volumes of the desired detergent concentration in the presence of buffer and then to elute the protein in a single step with 600 mM KCl in the same detergent concentration and buffer. We typically carried out experiments in a final concentration of 200 mM KCl and could therefore dilute the high eluant in 600 mM KCl with the appropriate solution to obtain the desired final concentrations of $^2\text{H}_2\text{O}$ and C14SB. Since the volumes required for sedimentation equilibrium are relatively small, we carried out this final column exchange step using small (0.5 ml–1 ml) bed volumes of the ion exchange resin and manually collected the eluant samples by counting drops (typically 13–18 drops per fraction) to avoid dilution of the eluted, detergent equilibrated samples.

2. Preparation of OMPLA Q94A

A single-point mutant of OMPLA, Q94A, was generated using standard molecular biology techniques. This protein was expressed and purified using the protocol for the wild-type protein. Before any experimentation, OMPLA Q94A was applied to a Q-sepharose column and eluted in column buffer with 600 mM KCl. The extinction coefficient used for both the WT and Q94A sequence variant was $90,444 \text{ M}^{-1} \text{ cm}^{-1}$ (Dekker *et al.*, 1995).

3. Preparation of OmpF Samples

a. Expression and Purification of OmpF

The coding sequence for the mature *Escherichia coli* OmpF protein was amplified via PCR from the *E. coli* strain DH5 α . To express the protein into inclusion bodies, PCR primers were designed to replace the signal sequence with a start codon (forward: 5'-G GCA GTA CAT ATG GCA GAA ATC TAT AAC AAA GAT GGC-3'; reverse: 5'-CG GGA TCC TTA CAA CTG GTA AAC GAT ACC

CAC AG-3'). The insert was cut and ligated into a pET11a expression vector (Novagen). This vector was transformed into *E. coli* BL21(DE3) cells and the nucleotide sequence was confirmed by DNA sequencing. Mature OmpF was purified from inclusion bodies using a published procedure (Dekker *et al.*, 1995). Washed inclusion body pellets were stored at -20°C until further use.

Inclusion body pellets of OmpF were resuspended in unfolding buffer (20 mM sodium phosphate, 8 M urea, pH 7.3). According to the folding conditions described by Surrey *et al.* (1996), OmpF (13.4 μM , final concentration) was added to the folding buffer (3.7 mM dodecylmaltoside, 3.7 mM dimyristoylphosphatidylcholine (DMPC), 20 mM sodium phosphate, pH 6.5) and incubated overnight at room temperature with gentle stirring. To exchange DMPC for detergent, C14SB was added to the folding conditions (20 mM, final concentration). OmpF was then applied to a UNO Q-1 column (BioRad), washed with column buffer (5 mM C14, 20 mM Tris-HCl, pH 8.3), and eluted in column buffer with 300 mM KCl. Thin-layer chromatography confirmed that DMPC was no longer associated with the protein (data not shown). To remove unfolded protein not inserted into micelles, OmpF was incubated overnight at 37°C in 0.02 mg/ml trypsin, followed by overnight dialysis against 300 mM KCl, 0.4 mM C14, 20 mM Tris-HCl, pH 8.3. If necessary, protein was concentrated on a Q-Sepharose column (Pharmacia) and eluted in column buffer with 1 M KCl.

The OmpF protein concentration was determined by absorbance at 280 nm using the extinction coefficient calculated by SEDNTERP (Laue *et al.*, 1992), $54,200\text{ M}^{-1}\text{ cm}^{-1}$. To determine the extinction coefficient of OmpF at 230 nm, protein absorbance was measured at both 230 and 280 nm and the average of the 230/280 ratio of six different samples was calculated to be 5.0. Therefore, the extinction coefficient used for OmpF at 230 nm was $271,000\text{ M}^{-1}\text{ cm}^{-1}$.

b. Vesicle Preparation for OmpF Folding

DMPC (Avanti Polar Lipids) dissolved in chloroform was placed under a gentle stream of N_2 gas and freeze-dried overnight to remove any residual chloroform. To hydrate the lipid, DMPC was resuspended in phosphate buffer (20 mM sodium phosphate, pH 6.5) to a final DMPC concentration of 14.75 mM and incubated at room temperature for at least 30 minutes with occasional vortexing. Unilamellar vesicles were prepared either by extrusion or sonication (Surrey *et al.*, 1996). For extrusion, hydrated DMPC was put through three freeze-thaw cycles in dry ice and 40°C water baths, followed by extrusion through a $0.1\ \mu\text{M}$ filter 11 times using the Avanti mini-extruder. Sonicated vesicles were prepared using a Branson Digital Sonifier for 50 minutes on a 50% duty cycle.

B. Determination of the Density-Matching Point for C14SB

A first step for all of these experiments was to determine the concentration of $^2\text{H}_2\text{O}$, which is required to density match the C14SB detergent micelles in the background of our other buffer components. To accomplish this, we carried out

sedimentation equilibrium experiments on 30 mM solutions of C14SB in 20 mM Tris-HCl, pH 8.0, and 200 mM KCl prepared in aqueous solutions containing $^2\text{H}_2\text{O}$ at 0%, 10%, 20%, and 30%. Reference samples contained all buffer components (including $^2\text{H}_2\text{O}$) but no detergent micelles. We used external loading 6-sector cells equipped with sapphire windows [(Ansevin *et al.*, 1970); also see Chapter 6 by Cole *et al.*, this volume] and collected interference buffer blanks on all cells prior to analyzing the detergent micelle samples; these scans were subsequently subtracted from the data scans and account for any radially independent, time-independent noise or slope in the interferograms. The sample volumes were 110 μl . We then removed the buffer from the sample side and loaded the detergent micelle solution. The interference optical system of a Beckman Optima XL-I was used to detect the distribution of micelles as a function of radius. We collected data at 50,000 rpm every 15 minutes and used the Windows version of Match to determine the time to equilibrium, which was generally less than 4 hours. We chose 50,000 rpm because this speed was faster than any of the speeds we anticipated using for our protein samples. Since detergents are more compressible than proteins, there is the formal possibility that any particular detergent would exhibit pressure effects; these would be reflected in a density gradient at high centrifugal forces. We reasoned that the absence of a density gradient at speeds much higher than what we would use for sedimentation equilibrium experiments would ensure its absence in our subsequent protein experiments at lower speeds. Over the course of the past 12 years of experiments, the author has never observed a pressure dependence with any protein or detergent sample; nevertheless, when initiating experiments with a new detergent it is prudent to check for an obvious presence of this in detergent samples. These detergent matching experiments were carried out at 25 $^\circ\text{C}$ because we anticipated using this temperature for the subsequent protein samples. We have not explored the temperature dependence of the match point for any of the detergents we have studied; however, we would recommend that an investigator determine the match point at the temperature of interest as it might be different.

Determination of the amount of $^2\text{H}_2\text{O}$ required to match the density of the detergent micelles requires analysis of the radial distributions of the detergent-only samples, and the shapes of the radial distributions for micelles in these density-matching experiments deserve comment. For detergents whose partial specific volumes fall between 0.9 and 1.0 ml g^{-1} , the effective molecular weights will be fairly low at the speeds attainable in the Beckman AUC instrument. The shapes of the experimentally obtained distributions are therefore extremely shallow exponentials and are in fact well described by the equation for a line. The slope of the line indicates relative densities of the micelles and the solution: if the detergent micelles are more dense than the solution, the slope will be positive; if the micelles are less dense than the solution, the slope will be negative (i.e., the micelles float); and at the isopycnic point, the slope is zero. Determination of the matching $^2\text{H}_2\text{O}$ concentration is therefore a simple matter of plotting the slope of the micelle distribution as a function of percent $^2\text{H}_2\text{O}$ and finding the point where the slope equals zero.

C. Sedimentation Equilibrium Experiments on Membrane Protein Samples Dispersed in C14SB

1. Sedimentation Equilibrium Conditions for OMPLA

Sedimentation equilibrium experiments were performed at 25 °C using a Beckman XL-A analytical ultracentrifuge. Samples were prepared in 100 mM KCl, 20 mM Tris-HCl, pH 8.3, 13% ²H₂O (the matching amount of ²H₂O). Initial protein concentrations corresponded to 0.9, 0.6, and 0.3 absorbance units at A₂₈₀, and the rotor speeds were 16,300, 20,000, and 24,500 revolutions per minute. In contrast to our earlier work on the dimeric GpA helix, we discovered in our early experiments that OMPLA has a modest propensity for self-association, and we therefore carried out the majority of our experiments in 5 mM C14SB. Increasing the concentration of detergent led to dilution of OMPLA in the detergent micelle phase and promoted dissociation of the OMPLA dimer. This detergent dependence made it impossible to determine interaction energetics as a function of detergent concentration since we could not simultaneously observe the OMPLA monomer and dimer at high detergent concentrations; under these conditions, only the monomer was populated.

2. Sedimentation Equilibrium Conditions for OmpF

Sedimentation equilibrium experiments on OmpF were performed at 25 °C using a Beckman XL-A analytical ultracentrifuge. Samples were prepared in either 100 or 200 mM KCl, 20 mM Tris-HCl, pH 8.3, 13% ²H₂O. Because of OmpF's pronounced trimeric stability, we collected sedimentation equilibrium data on OmpF at several different detergent micelle concentrations (5, 12, and 30 mM). To increase the probability of observing OmpF monomers and/or dimers, we also collected the data by monitoring the OmpF absorbance at 230 nm, which allowed us to observe a dilute protein solution. At each detergent concentration, we collected four speeds (9,000, 11,000, 13,500, and 16,300 rpm) and set up three initial protein concentrations corresponding to A₂₃₀ values of 0.3, 0.6, and 0.9; 12 equilibrium data sets were therefore collected in total.

Notably, the speeds used in the OmpF and OMPLA sedimentation equilibrium experiments differ. This is because the rotor speed should be chosen to optimize the exponential shape of the experimental data. As a rule of thumb, the lowest speed is chosen so that the effective molecular weight (σ) at that speed equals approximately unity, where the effective molecular weight is defined according to Yphantis (1964):

$$\sigma = \frac{M(1 - \bar{v}\rho)\omega^2}{RT} \quad (9)$$

where ω is the rotor speed in radians per second, R is the universal gas constant (8.314472 J mol⁻¹ K⁻¹), and T is the temperature in degrees Kelvin. Since the mass of the OmpF trimer is much larger than that of OMPLA, sedimentation equilibrium speeds are therefore lower for this protein. Subsequent speeds were chosen such

that the speed factor between any two speeds equals approximately 1.5; the speed factor is defined as

$$\text{Speed Factor} = \frac{\omega^2 \text{ for Speed2}}{\omega^2 \text{ for Speed1}} \quad (10)$$

Since the data will subsequently be globally fit to determine whether or not the macromolecules are reversibly self-associating, these speed choices ensure that the radial distributions of the protein will be significantly different from each other.

3. General Data Fitting Strategy

Typically, we collect three rotor speeds with three initial protein concentrations. This setup results in nine distinct radial distributions of the protein. Before analysis, each data set needs to be trimmed to extract the regions of the exponential distributions to be used for analysis, to remove the optical noise between the sectors in the cell, and to delete any bad points. The analyzable regions of the distributions start at a radial position just greater than that of the meniscus. Since the absorbance optical system is not linear with concentration above 1.2 on our instrument, we trim the data to end at an absorbance value no greater than this, and in cases where the concentration gradient at the bottom of the data set was high, the data were trimmed to lower maximum absorbance values. The freely available software program Winreedit is easy to use and can be employed in an iterative manner to trim data appropriately; data trimming can also be accomplished in the Sedanal preprocessor; alternatively, it can be carried out manually using almost any spreadsheet or data analysis program since the sedimentation equilibrium files are just ASCII text files. Importantly, the original files should always be backed up as the user may need to go back and reedit them at a future time.

Once data are trimmed, we globally fit each detergent concentration with either the Windows or the Mac OS9 version of NONLIN (Johnson *et al.*, 1981) by nonlinear least-squares curve fitting. The goal of the fitting process is to find the simplest model that describes the data: each set of data was initially fitted using a single ideal species model followed by fitting using equations describing increasingly complex reversible association schemes. The monomeric mass and partial specific volume of each of the proteins were calculated using the program SEDNTERP (Laue *et al.*, 1992) and the amino acid sequences as input. These values were held constant during fitting to self-association models.

D. Sedimentation Velocity Experiments on OmpF

For sedimentation velocity experiments, the absorbance optics were employed, and intensity scans were collected for protein in three different C14SB concentrations (5, 30, and 60 mM). The collection of intensity scans as opposed to default absorbance scans offered several advantages: First, it doubled the amount of data

that could be collected in the same time interval since both the reference and sample sectors of the cells could be loaded with samples; for example, we collected 6 data sets in 3 two-sector cells in a single experiment. Second, this data collection method offered an increase of $\sqrt{2}$ in the signal-to-noise ratio of each collected data set because the reference intensity data were not subtracted from the sample data. We processed and analyzed the data using SedAnal (Stafford and Sherwood, 2004), which can directly read the intensity scans and can correct for any time-independent offsets in the preprocessing step. Within SedAnal, the time-derivative method was used to determine the apparent sedimentation coefficient distribution, and the weight average sedimentation coefficient (s_w) for each data set were calculated by integration over the range of this distribution. All buffers contained 300 mM KCl and 20 mM Tris-HCl, pH 8.3. Note that there is no need or advantage to density match the detergent in sedimentation velocity experiments. The protein shape, bound water, and bound detergent will all contribute to the sedimentation coefficient. Moreover, because the sedimentation coefficient contains information about mass that is coupled to the frictional coefficient of the sedimenting particle, there is no way to deconvolute these factors.

E. Viscosity Measurements

The viscosities of buffers used in AUC experiments were determined on a Brookfield HA Model DV-III viscometer. The temperature was held at 25 °C with a water cooler (VWR). Two buffer samples were made for each detergent concentration, one with and the other without 2 mM EDTA. Three separate measurements were taken at 75, 150, and 250 rpm for each buffer. The presence or absence of 2 mM EDTA had no effect on the viscosity (data not shown). Therefore, the viscosity of the buffer at each detergent concentration was determined as the average of six different measurements, for example, readings of buffer with and without 2 mM EDTA at three different speeds.

F. Density Measurements

Buffers used in the SV experiments were filtered (0.22 μm pore) and degassed before their density was measured at 25 °C using an Anton Paar DMA 5000 density meter.

IV. Results

A. Analysis of OMPLA Dimerization Energetics

OMPLA is an outer membrane phospholipase enzyme found in gram-negative bacteria; it becomes activated when these organisms experience stress, and activity requires dimerization of the enzyme as well as calcium binding. The crystal

structures of OMPLA show that complete active sites and calcium binding sites are formed at the interface of the two monomers, explaining why dimerization is a prerequisite for enzyme activity. To understand the molecular basis of OMPLA activation, it is necessary to know how energetically favorable dimerization is as well as how the free energy of dimerization is affected by substrate binding and calcium binding. We therefore used sedimentation equilibrium to address this question (Stanley *et al.*, 2006, 2007), and we will use the example of OMPLA dimerization to illustrate in this chapter how a researcher would determine whether or not a system is reversibly associating in solution or alternatively is a mixture of irreversible aggregates. This distinction is important because the stoichiometry of the oligomeric species can be determined in both situations; however, the extraction of the equilibrium constant and an extrapolation of the population distribution over a wide concentration range can be carried out only when the system is reversibly associating on the timescale of the sedimentation equilibrium experiment.

We investigated the interaction energetics of OMPLA under four conditions: (1) in the absence of any cofactors; (2) in the presence of 20 mM CaCl_2 ; (3) in the presence of covalently bound substrate analog; and (4) in the presence of both covalently bound substrate analog and 20 mM CaCl_2 (Stanley *et al.*, 2006). The sedimentation equilibrium conditions—speeds, temperature, and detergent concentration—were identical for each of these samples; the only differences were the presence or absence of noncleavable substrate analog and calcium. Derivatization of OMPLA with the fatty acyl chain substrate analogue is described in detail in Stanley *et al.* (2006, 2007) and will not be further discussed here. For the purposes of illustrating how the analysis is carried out in this chapter, we will consider the sedimentation equilibrium profiles of OMPLA under conditions (1) and (4) from above.

1. OMPLA is Monomeric in the Absence of Cofactors

We first evaluated OMPLA in 5 mM C14SB in buffered solution with 20 mM EDTA. The extracted data sets were globally analyzed using the model for a single ideal species in which the molecular weight was a global fitting parameter that was allowed to float in the combined fit of all nine data sets. Under these buffer conditions, this mathematical model provided a good description of the OMPLA radial distributions as evidenced by a square root of the variance value on the order of the noise (~ 0.005 for our instrument) and residuals that were randomly distributed and centered on zero. A single data set from this global fit is shown in Fig. 1 where the residual distribution can be observed. The resultant molecular weight from this fit was within 5% of that predicted for monomeric OMPLA based on the amino acid sequence, and we therefore concluded that OMPLA was 100% monomeric at these concentrations and under these buffer conditions.

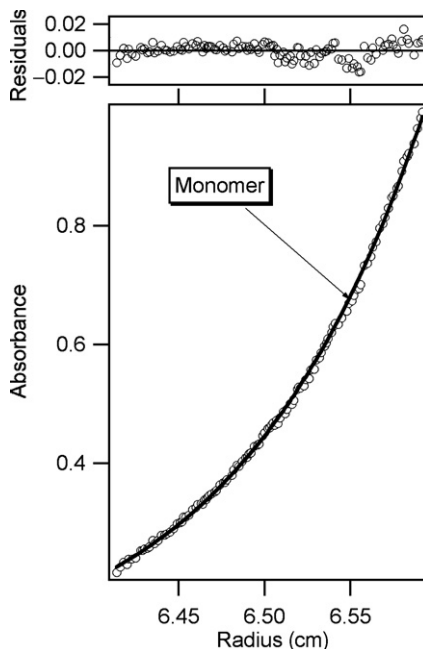


Fig. 1 Single-species fit of outer membrane phospholipase A (OMPLA) in the absence of substrate and CaCl_2 . A representative sedimentation equilibrium scan collected at 20,000 rpm is shown. The open circles in the lower panel show the data, and the line represents the fit to a single-species equation. The open circles in the upper panel represent the residuals of the fit, which are the differences between the fit and the data at each point.

2. OMPLA Participates in a Reversible Monomer–Dimer Equilibrium Reaction When Modified with Decylsulfonylfluoride but Not When Modified with Perfluorinated Octylsulfonylfluoride

The second condition that we consider in this chapter is OMPLA modified with an acyl chain analogue and in the presence of CaCl_2 . To explore the dependence of OMPLA dimerization on its substrate, we modified OMPLA with substrates composed of different acyl chain lengths and different chemical compositions (Stanley *et al.*, 2007). In this chapter, we will consider the data collected in the presence of two different substrates: (1) decylsulfonylfluoride (DSF), a 10-carbon acyl chain; and (2) perfluorinated octylsulfonylfluoride (pOSF), an 8-carbon acyl chain in which all hydrogen atoms have been replaced by fluorine atoms.

The setup for sedimentation equilibrium experiments of these samples was identical to that described for OMPLA in the absence of any cofactors. The data at the same three rotor speeds were collected on samples at initial protein concentrations corresponding to A_{280} values of 0.9, 0.6, and 0.3. The extracted data files were globally analyzed as before; however, the initial single ideal species fit returned values greater than that expected for a population composed entirely of

monomer (data not shown). We therefore fit the data to models describing multiple species in solution (e.g., monomer–dimer, monomer–trimer, monomer–tetramer). For these fits, we fix the value of sigma to that calculated for the monomer, and we allow the equilibrium constant for a particular monomer to vary in the global fit. The monomer–dimer fits are shown in Figs. 2 and 3 for the protein modified with DSF and pOSF, respectively. While the radial profiles in the bottom panels of these two figures are not obviously different, the ability of a global monomer–dimer fit to describe the data is markedly better for the DSF sample in Fig. 2 than it is for the pOSF sample in Fig. 3. The key comparative parameter is the distribution of the residuals. Since the residuals in Fig. 3 are nonrandom, we must conclude that the global monomer–dimer fit does not describe the data; this means that the equilibrium constant returned in that “fit” is not a valid description of the reaction

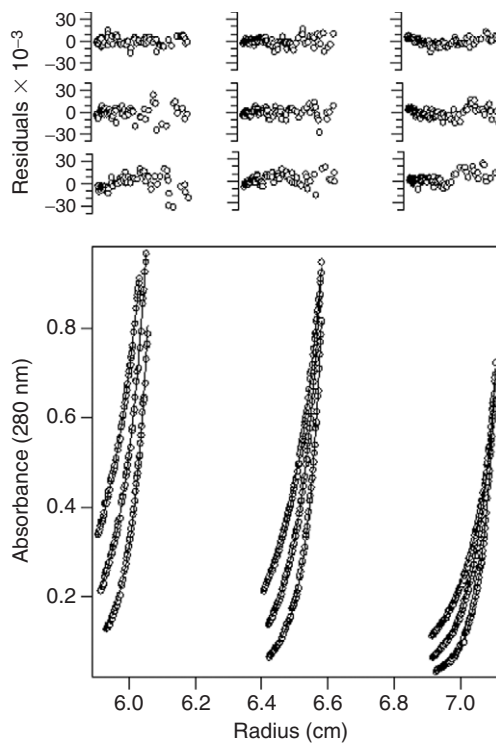


Fig. 2 Global fit analysis of outer membrane phospholipase A (OMPLA) in the presence of CaCl_2 and modified with decylsulfonylethylamine (DSF). The open circles in the lower panel are the data collected at three different concentrations (high to low from left to right) and at three different speeds (16,300, 20,000, and 24,500 rpm, more shallow to less shallow exponential for each concentration). The lines in the lower panel represent the global and simultaneous fit to all the data. The open circles in the upper panels represent the residuals of each fit. These are all randomly distributed around zero, suggesting that the monomer–dimer equation with a single equilibrium constant is a good description of the data.

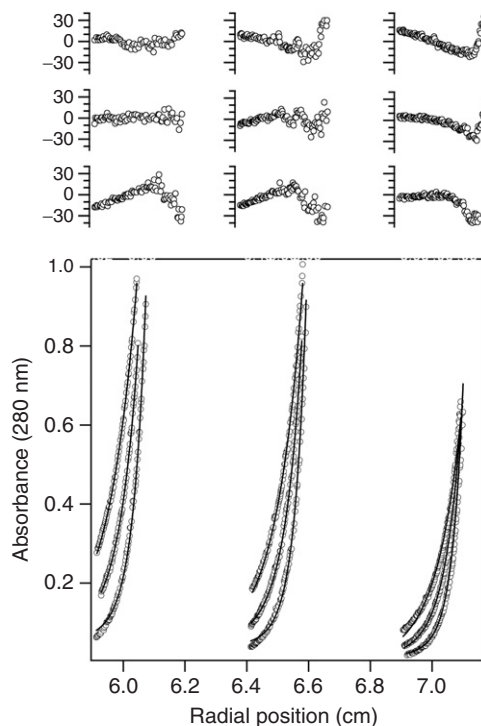


Fig. 3 Global fit analysis of outer membrane phospholipase A (OMPLA) in the presence of CaCl_2 and modified with perfluorinated octylsulfonylethylamine (pOSF). The open circles in the lower panel are the data collected at three different concentrations (high to low from left to right) and at three different speeds (16,300, 20,000, and 24,500 rpm, more shallow to less shallow exponential for each concentration). The lines in the lower panel represent the global and simultaneous fit to all the data. The open circles in the upper panels represent the residuals of each fit. In contrast to Fig. 2, the residuals in this figure are not randomly distributed around zero, suggesting that the monomer–dimer equation with a single equilibrium constant is not a good description of the data, which means that the monomer and dimer species are not reversibly associating on the timescale of the experiment and that no conclusions can be drawn about the thermodynamics of self-association.

and that pOSF stimulates aggregation—not reversible self-association—of OMPLA. Another possible conclusion is that the monomer–dimer model is not a correct description of the populated species when modified by pOSF. On the contrary, the residuals in Fig. 2 are randomly distributed in all data sets, suggesting that a single equilibrium constant can describe the reaction independent of the rotor speed and initial protein concentration; this means that the monomer and dimer are reversibly associating on the timescale of the experiment and that the fitted equilibrium constant is a measure of the thermodynamic activity of the solution. Notably, it is the power of the global fit that allows us to draw this conclusion. When analyzed individually, the monomer–dimer model (reversible

or irreversible) is a good fit *of any single data set*, and if we had only collected sedimentation equilibrium data at a single concentration and speed, we would not have been able to globally fit the data to test whether a protein sample contained irreversible aggregates or was participating in a reversible self-association reaction.

B. Analysis of OmpF Trimer Stability in C14SB

We also carried out experiments to determine the thermodynamic stability of the OmpF trimer in C14SB detergent micelles. The experimental setup was similar to that used in the OMPLA experiments; however, the rotor speeds were slower because of the higher molecular weight as described in [Section III](#). Since OmpF was also much more stable than OMPLA, we made two modifications to our experiments in order to try and populate monomer and/or dimers of OmpF with the goal of thermodynamically describing the assembly of the OmpF trimer: (1) We monitored the protein concentration at an absorbance wavelength of 230 nm instead of 280 nm. In general, proteins have a larger extinction coefficient at 230 nm, which allows one to experimentally access lower protein concentrations. As discussed in Chapter 6 by Cole *et al.*, this volume, it is a simple matter to change the detection wavelength on the Beckman Optima ultracentrifuges. (2) A second difference in the OmpF experiments is that we carried out sedimentation equilibrium experiments in several different detergent micelle concentrations. For each detergent concentration, we set up three initial protein concentrations and collected several speeds. Since integral membrane proteins are partitioned into the micellar phase of an aqueous solution, increasing the detergent concentration leads to dilution of the membrane protein within that phase, and we reasoned that increasing the detergent concentration would populate OmpF monomers and/or dimers if the concentration went below the dissociation constant. We previously showed using the GpA helix–helix dimer that a reversible membrane protein interaction responds to the aqueous detergent concentration in a predictable way if the solution is behaving ideally ([Fleming, 2002](#); [Fleming *et al.*, 2004](#)), and changing the detergent concentration would further allow us to test this for OmpF.

We globally fit OmpF sedimentation equilibrium data collected for each detergent concentration (5, 12, or 30 mM) at four different speeds (9000, 11,000, 13,500, and 16,300 rpm) and three different initial protein concentrations. A representative data set from the global fit is shown in [Fig. 4A](#) and illustrates the good single ideal species fit. This fit returned a molecular weight of $105,000 \pm 1,000$ Da, which is $6 \pm 1\%$ lower than the calculated molecular weight for a trimer (111,000 Da) and just below the limit for the expected molecular weight accuracy of sedimentation equilibrium ($\pm 5\%$). There are two interpretations of these initial sedimentation equilibrium fits. First, OmpF is completely trimeric under these conditions and that the calculated molecular weight is slightly inaccurate. If so, we speculate that this inaccuracy arises from uncertainties in our calculation of the partial specific volume of the OmpF trimer, which we assume is an additive function of the partial

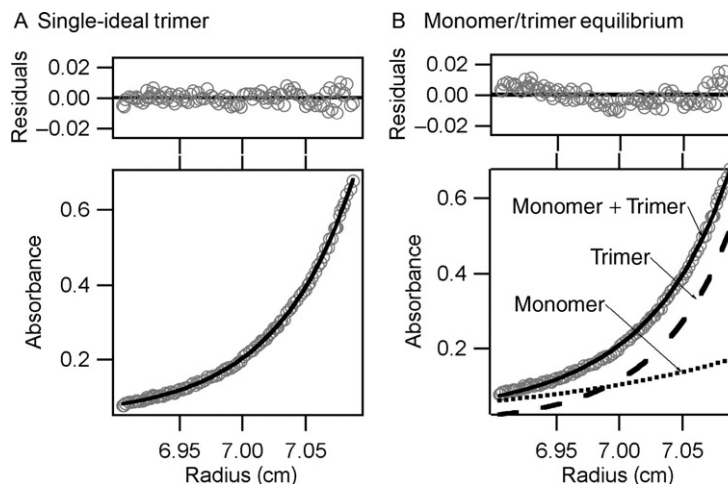


Fig. 4 Outer membrane protein F (OmpF) is a single-species trimer. A representative sedimentation equilibrium scan collected at 13,500 rpm of OmpF (11.1 μM , initial concentration) in 12 mM C14SB, 100 mM KCl, 20 mM Tris-HCl, pH 8.3. Both (A) and (B) show the same data fit with different models. The bottom panels show the observed absorbance (open circles) as a function of radius. The solid line shows the respective fits and the residuals of each fit are displayed in the top panels. (A) Data fit with a single-ideal-species model. The residuals (top panel) fall randomly and tightly about the fit, suggesting that the single-ideal-species model describes the data well. (B) Data fit with a reversibly associating monomer-trimer model. The relative contributions to the fit (solid line) by the monomer and trimer species present are shown by the dotted line (monomer) and dashed line (trimer). The residuals (top panel) of this fit show a curved trend and are greater in magnitude than the residuals of the single-ideal-species model and demonstrate that the monomer-trimer model does not describe the data better than the single-ideal-species model.

specific volumes for each of the OmpF monomers; alternatively, there could be a slight change in the density of the detergent once it is bound to OmpF. It is well known (for a $\bar{v} = 0.75 \text{ ml g}^{-1}$) that each 1% error in the partial specific volume propagates to a 3% error in the buoyant molecular weight; therefore, even a small deviation of this value from the calculated one can lead to an uncertainty in data interpretation. In principle, it is possible to experimentally determine the partial specific volume of a soluble protein from density measurements, but this would not work as well for a membrane protein since the density measurement would contain contributions from the bound detergent as well as the protein. A second interpretation for the slight decrease in the experimentally observed molecular weight of the OmpF trimer may be that the trimer exists in an equilibrium species of lower molecular weight. One of the advantages of sedimentation equilibrium is that it can be sensitive to components present at levels of only 5–10%. While we anticipated that the OmpF trimer would be quite stable, we were also interested to know whether we could experimentally access a reversible equilibrium between OmpF trimers and monomers or dimers.

To test this hypothesis we fit the data with models that account for multiple species. The possibility of a population of only monomers and/or dimers was eliminated because the results of a single ideal species fit demonstrated that the effective molecular weight was significantly higher than that expected for an OmpF dimer. We therefore fit the data to three other models representing association between (1) monomers and trimers, (2) monomers and tetramers, and (3) monomers, dimers, and trimers. Global fits produced with multiple-species models did not significantly decrease the square root of variance over the single-ideal-species model (data not shown). The relative quality of the fits with different models is further evident when fitting individual data sets (Fig. 4). The residuals of multiple-species models fits (Fig. 4B) either did not change from or were less random than residuals of a single-species fit (Fig. 4A). Comparing the residuals of the individual data sets and the square root of variance of the global fits reveals that the multiple-species models do not fit the data better than the single-ideal-species model. We therefore concluded that the sedimentation equilibrium data are best described by a single-species trimer.

C. Sedimentation Velocity Experiments on OmpF

To obtain independent experimental data for the single-species trimer model of OmpF, we carried out sedimentation velocity experiments. Because of the manner in which the data are analyzed, sedimentation velocity methods facilitate experiments at lower protein concentrations, which should further populate OmpF monomers and/or dimers if they are in fact in a reversible equilibrium with the OmpF trimer observed in the sedimentation equilibrium experiments. Since OmpF dimers have been observed at lower protein concentrations (Watanabe and Inoko, 2005), we postulated that sedimentation velocity experiments might allow observation of OmpF dissociation.

Furthermore, Stafford has shown that s_w is a measure of the thermodynamic activity of a macromolecule in solution (Stafford, 2000). For self-associating soluble proteins, s_w will decrease with decreasing protein concentration if the protein dissociates. A plot of s_w versus the protein concentration can be fit with an equation describing a binding isotherm to determine the association constant for the equilibrium reaction (Correia, 2000). However, it is essential to recognize that the concentration scales for soluble and membrane proteins should be fundamentally different for this type of analysis. In contrast to soluble proteins, the mass action behavior of membrane proteins will not depend on the aqueous concentration but rather will depend on the protein:detergent mole ratio (referred to as the mole fraction protein) as the concentration unit. This is extensively discussed by Fleming and has its origins in the fact that folded membrane proteins do not partition into an aqueous environment (Fleming, 2002).

Analysis of any one of the sets of sedimentation velocity scans revealed a single peak in the apparent s_w distribution. This is illustrated by the data in Fig. 5. Because of the mass and shape contribution of bound detergent molecules,

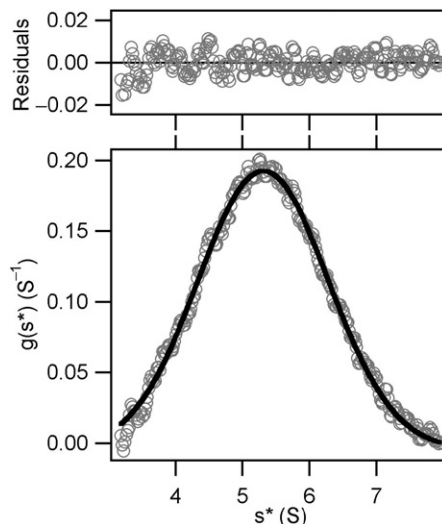


Fig. 5 Sedimentation velocity profile of outer membrane protein F (OmpF). Analysis of a representative sedimentation velocity scan of $11.1 \mu\text{M}$ OmpF in 60 mM C14SB. The bottom panel displays the apparent sedimentation coefficient distribution, $g(s^*)$ versus s^* (open circles), which was calculated from the time derivative of the raw data. The error bars from this calculation were no larger than the markers used here and were therefore left out for greater graphical clarity. The single peak produced by this analysis reflects either a single species or the weight average of several species in equilibrium with each other. The mean of a Gaussian fit (black line) defines the weight average sedimentation coefficient (s_w). The top panel displays the residuals of the fit, which are small and random, demonstrating a good fit.

the theoretical sedimentation coefficient for a membrane protein cannot be calculated from either its composition or its crystal structure; this means that the single experimental peak can be interpreted as a single species or as the reaction boundary of multiple species in equilibrium. To distinguish between these single- and multiple-species models, we carried out sedimentation velocity experiments as a function of the mole fraction protein concentration. We varied both the aqueous protein and detergent concentrations to obtain several different protein mole fractions. Like the representative data in Fig. 5, each of these could be fit to a single sedimentation coefficient. The s_w values observed in our experiments ranged from 5.3 to 5.8 S (Fig. 6A). Notably, these values are consistent with previously published sedimentation coefficients of the OmpF trimer in other lipidic environments, such as in lipopolysaccharide ($s=5.0 \text{ S}$) (Holzenburg *et al.*, 1989), in octylglucopyranoside micelles ($s=6.2 \text{ S}$, 6.4 S , and 6.6 S) (Lustig *et al.*, 2000; Markovic-Housley and Garavito, 1986), and in sodium dodecylsulfate micelles ($s=6.0 \text{ S}$) (Markovic-Housley and Garavito, 1986). However, a plot of the observed s_w values as a function of mole fraction protein does in fact reveal a trend that has a shape similar to a binding isotherm: s_w decreases with lower mole fraction protein (Fig. 6A). The trend may illustrate the effect of increasing buffer

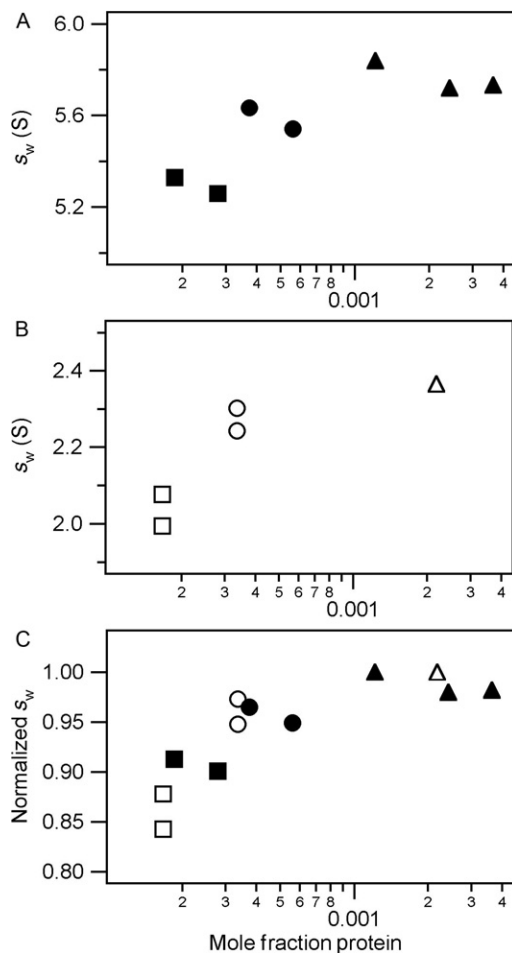


Fig. 6 Outer membrane protein F (OmpF) behaves as a single species despite the hyperbolic shape of the sedimentation coefficient concentration dependence. Results of sedimentation velocity experiments with (A) OmpF and (B) outer membrane phospholipase A (OMPLA) Q94A at various C14SB concentrations: 5 mM (triangles), 30 mM (circles), and 60 mM (squares). The apparent s_w is plotted as a function of mole fraction protein. (C) The values of s_w were normalized with respect to the largest s_w for each protein. The normalized s_w for OmpF (closed markers) and OMPLA Q94A (open markers) are plotted as a function of mole fraction protein.

density or viscosity at high detergent concentrations on the sedimentation coefficient of a single-species. Alternatively, the decrease in s_w might indicate the presence of multiple species undergoing more dissociation at greater detergent concentrations.

To determine if the variation of the s_w resulted from dissociation, we used the OMPLA sequence variant Q94A as a control for sedimentation velocity

experiments. Under the same experimental conditions used for OmpF, it is known that wild-type OMPLA (Stanley *et al.*, 2006) and the sequence variant Q94A are monomeric. In the sedimentation velocity experiments with the OMPLA variant Q94A, we also observed a distribution ($s_w=2.0-2.4$ S). In Fig. 6B, s_w is plotted as a function of mole fraction protein and demonstrates that the s_w of OMPLA Q94A decreased as a function of mole fraction protein, similar to the trend observed for OmpF.

The differences in the absolute values of s_w obtained for OmpF ($s_w=5.3-5.8$ S) and OMPLA Q94A ($s_w=2.0-2.4$ S) are not surprising because of the difference in molecular weight of the OmpF trimer (111,000 Da) and the OMPLA Q94A monomer (31,000 Da). To compare the trends in the distribution of s_w , the values were normalized to the highest observed for each protein. The normalized s_w values were then plotted as a function of mole fraction protein (Fig. 6C). The trend observed for the OmpF trimer in Fig. 6C overlays that of OMPLA Q94A, a completely monomeric protein. This result indicates that the detergent dependence of s_w observed in OmpF cannot be explained by the dissociation of the OmpF trimer into monomers in dilute conditions; rather these data support the conclusions drawn from the sedimentation equilibrium data: OmpF is a single-species trimer.

The variation in s_w for a single species was unexpected, so we explored the probability that the variation resulted from changes in bulk solvent properties. Sedimentation velocity experiments quantify the hydrodynamic properties of macromolecules, so changes in the buffer viscosity or density at high detergent concentrations could contribute to the observed behavior of both OmpF and OMPLA. To determine whether bulk solvent properties affect the s_w distribution, we measured the viscosity and density of all buffers in the absence of protein. We found that the viscosity and density of the buffers do not change over the detergent concentrations used nor do they vary significantly from the calculated values of the buffer without detergent (Fig. 7). Therefore, changes in bulk solvent properties do not likely account for variation in the measured s_w .

Apart from bulk solvent properties, s_w is also sensitive to the size and shape of the macromolecule. The number of detergent molecules bound to the protein may affect both the size and the shape of a detergent-protein complex. For example, Watanabe and Inoko observed through small angle light scattering that the OmpF dimer-micelle complex and the trimer-micelle complex are of the same size. They concluded that the variation in the amount of detergent bound accounted for the difference in size between the dimer and the trimer (Watanabe and Inoko, 2005). Similarly, the number of detergents bound to OmpF may have varied between our experiments. If the number of detergent molecules varied with the detergent concentration (the only parameter that changed between sedimentation velocity experiments), then s_w would also vary with detergent concentration and account for the observed trend. However, the number of detergent molecules that solvate a given membrane protein is generally not known; neither can it be concluded whether that number varies at different detergent concentrations. Although the

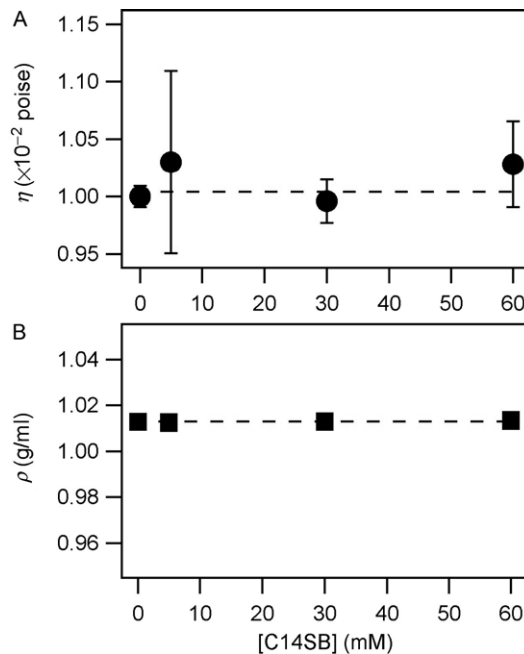


Fig. 7 Viscosity and density of buffers do not change with detergent concentration. (A) The buffer viscosity is plotted as a function of C14SB detergent concentration. The error bars represent the standard deviation of six independent measurements. (B) The buffer density of two independent measurements at each detergent concentration is plotted as a function of C14SB concentration. The viscosity and density of the buffers in the absence of detergent were determined in SEDNTERP (Laue *et al.*, 1992) and are shown in both panels as a dashed horizontal line.

structure of the protein–detergent micelle complex is not yet understood, we have shown that for β -barrel membrane proteins, the change in s_w with mole fraction protein is not necessarily a reflection of the law of mass action or an indication of the dissociation of oligomers. Sedimentation-velocity studies of detergent-solvated membrane proteins should be interpreted carefully.

===== V. Discussion

Knowledge of the thermodynamic stabilities of several membrane proteins makes it possible to rank a set of proteins by their interaction energies. This is illustrated by Fig. 8 in which relative oligomeric populations of several membrane proteins, OmpF, GpA (Fleming *et al.*, 2004), and OMPLA, with and without effector molecules (Stanley *et al.*, 2006) are plotted as a function of mole fraction protein. “Mole fraction protein” was chosen as the quantity for the abscissa for

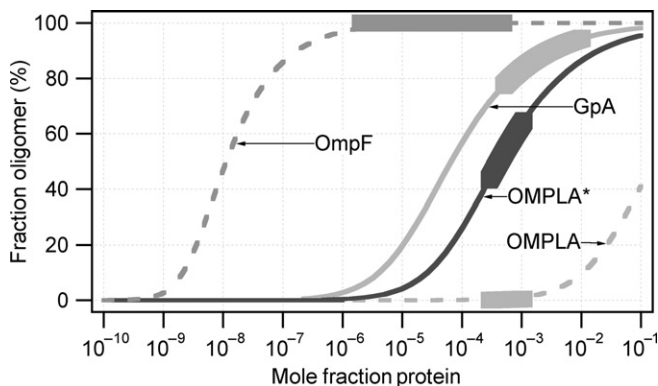


Fig. 8 A comparison of the oligomer populations for several membrane proteins. The fraction oligomers of OmpF, GpA, outer membrane phospholipase A (OMPLA) with effector molecules (*) (purple), and OMPLA without effector molecules are plotted as a function of mole fraction protein. The thick portions of the curve represent the observed oligomeric populations from which the standard-state free energies were calculated (Fleming *et al.*, 2004; Stanley *et al.*, 2006). No monomeric species for OmpF nor oligomeric species for OMPLA without effector molecules (Stanley *et al.*, 2006) were observed and therefore the dashed curves represent limits to the free energy of association. Under all observed conditions, both GpA and OMPLA self-association is much weaker than OmpF self-association.

this comparison as this concentration scale represents the distributions of the membrane proteins within the micellar phase (Fleming, 2002). Mole fraction protein is defined as the ratio of the aqueous molar concentrations of protein to micellar detergent. The mole fraction scale normalizes the observed equilibrium constant to the detergent micelle concentration used in any particular experiment and allows a direct comparison of membrane protein populations even if the data were collected in different detergent concentrations. Underlying the mole fraction representation of the data is the assumption that the membrane protein is behaving ideally within the micellar phase, and it is important to recognize that this condition has been experimentally demonstrated only for the GpA helix dimer (Fleming *et al.*, 2004); it is an assumed behavior for the other proteins on this graph. The thin lines in Fig. 8 show the predicted change in fraction oligomer as a function of mole fraction protein and were calculated from the dissociation constants of the observed oligomeric populations (thick portion of the lines) as measured by sedimentation equilibrium experiments (Fleming *et al.*, 2004; Kobus and Fleming, 2005; Stanley *et al.*, 2006). OmpF was detected as a single-species trimer over the experimentally accessible mole fraction protein, and we therefore calculated an estimate of upper limit for the dissociation constant. Assuming a cooperative trimer-to-monomer dissociation scheme, we forced the fraction oligomer to decrease from the lowest experimentally observed mole fraction protein. The theoretical curve for OmpF represents the upper limit to the mole fraction

concentration that would dissociate an OmpF trimer; in reality, the OmpF trimer may be more stable than the distribution shown in Fig. 8. Similarly, there was no dimeric population observed for OMPLA without effector molecules (Stanley *et al.*, 2006); thus, the reported value for the free energy of association of OMPLA is also a limit and reflects the most favorable self-association that might exist. To date, these curves define the limits of the free energy of association for β -barrel membrane proteins.

An estimate of the increased stability of the OmpF trimer over the other membrane proteins can also be expressed numerically by calculating the free energy from the association constants that the curves in Fig. 8 represent. For OmpF, the sedimentation equilibrium data suggest that the highest limit of the standard-state free energy of association is $-26 \text{ kcal mol}^{-2}$. The standard-state free energy of association observed for GpA is $-5.7 \text{ kcal mol}^{-1}$ (Fleming *et al.*, 2004), for OMPLA with effector molecules is $-4.2 \text{ kcal mol}^{-1}$, and for OMPLA without effector molecules is $-1.05 \text{ kcal mol}^{-1}$ (Stanley *et al.*, 2006). These thermodynamic values illustrate the wide range of stabilities that can be encoded in membrane proteins, and it will be interesting in the future to compare these to the stabilities of additional membrane proteins.

VI. Summary

AUC is a powerful method that can be used to derive quantitative descriptions of membrane protein complexes dispersed in detergent micelle solutions. Using the density-matching method, the molecular weights of membrane proteins can be unequivocally determined, and global analysis of sedimentation equilibrium data can reveal whether membrane proteins are reversibly associating in detergent micelle solutions. When reversible association is established, the equilibrium constant can be extracted, and this quantity can be used to predict the species population over a wide range of protein concentrations. Knowing the thermodynamic stability of membrane proteins in the same detergent micelle environment allows a comparison of the population distributions and provides a basis for understanding how the sequences and the structures of membrane proteins encode their stabilities and functions.

Acknowledgments

This work was supported by a grant from the NSF (MCB0423807). Ann Marie Stanley is a Howard Hughes predoctoral fellow. We gratefully acknowledge Dr. John J. Correia at the University of Mississippi Medical Center AUC facility for the density measurements and for a critical reading of the manuscript, Dr. Richard Cone for access to a viscometer, and Elizabeth O'Hanlon for technical assistance. We also thank members of the Fleming lab for helpful discussions.

References

- Ansevin, A., Roark, D., and Yphantis, D. (1970). Improved ultracentrifuge cells for high speed sedimentation equilibrium studies with interference optics. *Anal. Biochem.* **34**, 237–261.
- Burrows, S., Doyle, M., Murphy, K., Franklin, S., White, J., Brooks, I., McNulty, D., Miller, S., Knutson, J., Porter, D., Young, P., and Hensley, P. (1994). Determination of the monomer-dimer equilibrium of interleukin-8 reveals it is a monomer at physiological concentrations. *Biochemistry* **33** 12741–12745.
- Butler, P. J., and Kuhlbrandt, W. (1988). Determination of the aggregate size in detergent solution of the light-harvesting chlorophyll a/b-protein complex from chloroplast membranes. *Proc. Natl. Acad. Sci. USA* **85**, 3797–3801.
- Butler, P. J., Ubarretxena-Belandia, I., Warne, T., and Tate, C. G. (2004). The *Escherichia coli* multidrug transporter EmrE is a dimer in the detergent-solubilised state. *J. Mol. Biol.* **340**, 797–808.
- Casassa, E. F., and Eisenberg, H. (1964). Thermodynamic analysis of multicomponent systems. *Adv. Protein Chem.* **19**, 287–395.
- Correia, J. (2000). Analysis of weight average sedimentation velocity data. *Methods Enzymol.* **321**, 81–100.
- Dekker, N., Merck, K., Tommassen, J., and Verheij, H. M. (1995). *In vitro* folding of *Escherichia coli* outer-membrane phospholipase A. *Eur. J. Biochem.* **232**, 214–219.
- Dekker, N., Tommassen, J., Lustig, A., Rosenbusch, J. P., and Verheij, H. M. (1997). Dimerization regulates the enzymatic activity of *Escherichia coli* outer membrane phospholipase A. *J. Biol. Chem.* **272**, 3179–3184.
- Doura, A. K., and Fleming, K. G. (2004). Complex interactions at the helix-helix interface stabilize the glycoprotein A transmembrane dimer. *J. Mol. Biol.* **343**, 1487–1497.
- Doura, A. K., Kobus, F. J., Dubrovsky, L., Hibbard, E., and Fleming, K. G. (2004). Sequence context modulates the stability of a GxxxG mediated transmembrane helix-helix dimer. *J. Mol. Biol.* **341**, 991–998.
- Doyle, D. A., Cabral, J. M., Pfuetzner, R. A., Kuo, A., Gulbis, J. M., Cohen, S. L., Chait, B. T., and MacKinnon, R. (1998). The structure of the potassium channel: Molecular basis of K⁺ conduction and selectivity. *Science* **280**, 69–77.
- Durshlag, H. (1986). Specific volumes of biological macromolecules and some other molecules of biological interest. In “Thermodynamic Data for Biochemistry and Biotechnology” (H. J. Hinz, ed.), pp. 45–128. Springer-Verlag, Berlin.
- Ebie, A. Z., and Fleming, K. G. (2007). Dimerization of the erythropoietin receptor transmembrane domain in micelles. *J. Mol. Biol.* **366**, 517–524.
- Fleming, K. G. (1998). Measuring transmembrane α -helix energies using analytical ultracentrifugation. In “Chemtracts: Biological Applications of the Analytical Ultracentrifuge” (J. C. Hanson, ed.), pp. 985–990. Springer-Verlag, New York.
- Fleming, K. G. (2000). Probing the stability of helical membrane proteins. *Methods Enzymol.* **323**, 63–77.
- Fleming, K. G. (2002). Standardizing the free energy change of transmembrane helix-helix interactions. *J. Mol. Biol.* **323**, 563–571.
- Fleming, K. G., and Engelman, D. M. (2001). Specificity in transmembrane helix-helix interactions defines a hierarchy of stability for sequence variants. *Proc. Natl. Acad. Sci. USA* **98**, 14340–14344.
- Fleming, K. G., Ackerman, A. L., and Engelman, D. M. (1997). The effect of point mutations on the free energy of transmembrane α -helix dimerization. *J. Mol. Biol.* **272**, 266–275.
- Fleming, K. G., Ren, C. C., Doura, A. K., Kobus, F. J., Easley, M. E., and Stanley, A. M. (2004). Thermodynamics of glycoprotein A transmembrane helix-helix association in C14 betaine micelles. *Biophys. Chem.* **108**, 43–49.
- Gratkowski, H., Lear, J. D., and DeGrado, W. F. (2001). Polar side chains drive the association of model transmembrane peptides. *Proc. Natl. Acad. Sci. USA* **98**, 880–885.
- Holzenburg, A., Engel, A., Kessler, R., Manz, H. J., Lustig, A., and Aebi, U. (1989). Rapid isolation of OmpF porin-LPS complexes suitable for structure-function studies. *Biochemistry* **28**, 4187–4193.

- Howard, K. P., Lear, J. D., and DeGrado, W. F. (2002). Sequence determinants of the energetics of folding of a transmembrane four-helix-bundle protein. *Proc. Natl. Acad. Sci. USA* **99**, 8568–8572.
- Johnson, M. L., Correia, J. J., Yphantis, D. A., and Halvorson, H. R. (1981). Analysis of data from the analytical ultracentrifuge by nonlinear least-squares techniques. *Biophys. J.* **36**, 575–588.
- Kobus, F. J., and Fleming, K. G. (2005). The GxxxG-containing transmembrane domain of the CCK4 oncogene does not encode preferential self-interactions. *Biochemistry* **44**, 1464–1470.
- Kochendoerfer, G. G., Salom, D., Lear, J. D., Wilk-Orescan, R., Kent, S. B., and DeGrado, W. F. (1999). Total chemical synthesis of the integral membrane protein influenza A virus M2: Role of its C-terminal domain in tetramer assembly. *Biochemistry* **38**, 11905–11913.
- Konig, N., Zampighi, G. A., and Butler, P. J. (1997). Characterisation of the major intrinsic protein (MIP) from bovine lens fibre membranes by electron microscopy and hydrodynamics. *J. Mol. Biol.* **265**, 590–602.
- Laue, T. M., Shah, B., Ridgeway, T. M., and Pelletier, S. L. (1992). Computer-aided interpretation of analytical sedimentation data for proteins. In “Analytical Ultracentrifugation in Biochemistry and Polymer Science” (S. E. Harding, A. J. Rowe, and J. C. Horton, eds.), pp. 90–125. Royal Society of Chemistry, Cambridge, UK.
- le Maire, M., Champeil, P., and Møller, J. V. (2000). Interaction of membrane proteins and lipids with solubilizing detergents. *Biochim. Biophys. Acta* **1508**, 86–111.
- le Maire, M., Kwee, K., Anderson, J. P., and Møller, J. V. (1983). Mode of interaction of polyoxyethylene-glycol detergents with membrane proteins. *Eur. J. Biochem.* **129**, 525–532.
- Li, R., Gorelik, R., Nanda, V., Law, P. B., Lear, J. D., DeGrado, W. F., and Bennett, J. S. (2004). Dimerization of the transmembrane domain of Integrin alphaIIb subunit in cell membranes. *J. Biol. Chem.* **279**, 26666–26673.
- Ludwig, B., Grabo, M., Gregor, I., Lustig, A., Regenass, M., and Rosenbusch, J. P. (1982). Solubilized cytochrome c oxidase from *Paracoccus denitrificans* is a monomer. *J. Biol. Chem.* **257**, 5576–5578.
- Lustig, A., Engel, A., Tsiotis, G., Landau, E. M., and Baschong, W. (2000). Molecular weight determination of membrane proteins by sedimentation equilibrium at the sucrose or nycodenz-adjusted density of the hydrated detergent micelle. *Biochim. Biophys. Acta* **1464**, 199–206.
- Markovic-Housley, Z., and Garavito, R. M. (1986). Effect of temperature and low pH on structure and stability of matrix porin in micellar detergent solutions. *Biochim. Biophys. Acta* **869**, 158–170.
- Pinto, L. H., Dieckmann, G. R., Gandhi, C. S., Papworth, C. G., Braman, J., Shaughnessy, M. A., Lear, J. D., Lamb, R. A., and DeGrado, W. F. (1997). A functionally defined model for the M2 proton channel of influenza A virus suggests a mechanism for its ion selectivity. *Proc. Natl. Acad. Sci. USA* **94**, 11301–11306.
- Reynolds, J. A., and McCaslin, D. R. (1985). Determination of protein molecular weight in complexes with detergent without knowledge of binding. *Methods Enzymol.* **117**, 41–53.
- Reynolds, J. A., and Tanford, C. (1976). Determination of molecular weight of the protein moiety in protein-detergent complexes without direct knowledge of detergent binding. *Proc. Natl. Acad. Sci. USA* **73**, 4467–4470.
- Stafford, W. F. (2000). Analysis of reversibly interacting macromolecular systems by time derivative sedimentation velocity. *Methods Enzymol.* **323**, 302–325.
- Stafford, W. F., and Sherwood, P. J. (2004). Analysis of heterologous interacting systems by sedimentation velocity: Curve fitting algorithms for estimation of sedimentation coefficients, equilibrium and kinetic constants. *Biophys. Chem.* **108**, 231–243.
- Stanley, A. M., and Fleming, K. G. (2005). The transmembrane domains of the ErbB receptors do not dimerize strongly in micelles. *J. Mol. Biol.* **347**, 759–772.
- Stanley, A. M., Chauwang, P., Hendrickson, T. L., and Fleming, K. G. (2006). Energetics of outer membrane phospholipase A (OMPLA) dimerization. *J. Mol. Biol.* **358**, 120–131.
- Stanley, A. M., Treubodt, A. M., Chauwang, P., Hendrickson, T. L., and Fleming, K. G. (2007). Lipid chain selectivity by outer membrane phospholipase A. *J. Mol. Biol.* **366**, 461–468.
- Suarez, M. D., Revzin, A., Narlock, R., Kempner, E. S., Thompson, D. A., and Ferguson-Miller, S. (1984). The functional and physical form of mammalian cytochrome c oxidase determined by gel

- filtration, radiation inactivation, and sedimentation equilibrium analysis. *J. Biol. Chem.* **259**, 13791–13799.
- Surrey, T., Schmid, A., and Jahnig, F. (1996). Folding and membrane insertion of the trimeric beta-barrel protein OmpF. *Biochemistry* **35**, 2283–2288.
- Watanabe, Y., and Inoko, Y. (2005). Physicochemical characterization of the reassembled dimer of an integral membrane protein OmpF porin. *Protein J.* **24**, 167–174.
- Yphantis, D. A. (1964). Equilibrium ultracentrifugation of dilute solutions. *Biochemistry* **3**, 297–317.